A Negative reactivity feedback driven by induced buoyancy after a temperature transient in lead-cooled fast reactors

Francisco J. Arias*

Department of Fluid Mechanics, University of Catalonia
ESEIAAT C/ Colom 11, 08222 Barcelona, Spain

Abstract

Consideration is given to the possibility to use changes in buoyancy as a negative reactivity feedback mechanism during temperature transients in heavy liquid metal fast reactors (HLMFRs). It is shown that by the proper use of heavy pellets in the fuel elements, fuel rods could be endowed with a passive self-ejection mechanism and then with a negative feedback. A first estimate of the feasibility of the mechanism is calculated by using a simplified geometry and model. If in addition, a neutron poison pellet is introduced in the bottom of the fuel, then when the fuel element is displaced upward by buoyancy force, the reactivity will be reduced not only by disassembly of the core but also by introducing the neutron poisson from the bottom. The use of induced buoyancy opens up the possibility of introducing greater amounts of actinides into the core, as well as providing a palliative solution to the problem of positive coolant temperature reactivity coefficients that could be featured by the HLMFRs.

Keywords: Heavy liquid metal fast reactors, buoyancy, Generation IV reactors

1. Introduction

Owing to the very high density of the coolant in HLMFRs similar to that of the fuel, it could be plausible to harness this unique feature of this kind or

*Corresponding author
Email address: francisco.javier.arias@upc.edu (Francisco J. Arias)

reactors to induce the disassembly of the core driven by temperature changes.

The objective of this study is to assess the potential for exploiting changes in buoyancy forces as a control mechanism for fuel rod self-ejection during HLMFR temperature transients, thereby providing a reliable solution to the well-established problem of the positive coolant temperature reactivity coefficient exhibited by fast reactors.

The effect of buoyancy forces in HLMFRs as a positive aspect in safety analysis during a post-accident heat removal scenario was recently investigated by Arias [3]. It was found that, because of the similar densities of the fuel and the heavy liquid metal (HLM) coolant, an inherent passive safety feedback self-removal mechanism governed by buoyancy is developed, propelling the packed bed away from the wall, and preventing temperatures that could jeopardize the structural integrity of the vessel being reached, as well as reducing the re-criticality potential by limiting the allowable bed depth.

Thus, it is interesting to consider whether buoyancy forces, rather than being regarded as a nuisance during nominal operating conditions, can be harnessed as a mechanism for endowing fuel rods with unique safety properties only available in HLMFRs. In the sections that follow, this possibility will be investigated and discussed. However, the reader should be aware that the results reported in this preliminary analysis of the proposed concept are based on idealizations, of the sort which are inevitable in preliminary theoretical assessments of concepts, and therefore should not be misconstrued as definitive detailed analysis. The final verdict about the feasibility of the proposed concept will only be reached following detailed analysis of the complexities arising from the proposed solutions, the subject of future work. Nonetheless, we feel that this preliminary assessment is appropriate at this time, to encourage (or not) further careful investigation of the idea.

2. Buoyancy forces as a fuel rod ejection mechanism

Fig. 1 illustrates schematically the mechanism we seek to exploit. For the envisaged mechanism to work as intended the density of the coolant needs to become greater than the effective density of the fuel as the temperature increases.

Fig. 2 shows the variation of density as a function of temperature for mixed oxide (MOX) and UO_2 fuels and Pb-Bi eutectic and Pb coolants. This indicates that the relative changes of HLM coolant and fuel densities

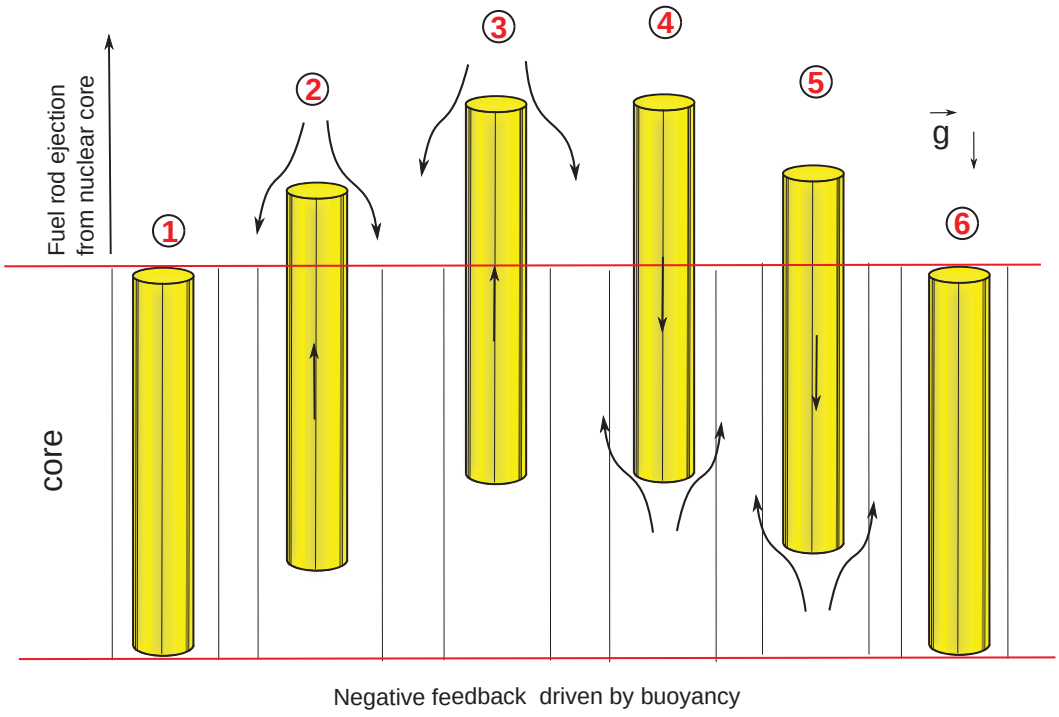

Fig. 1. Fuel rod ejection by buoyancy forces. Sequence: **(1)** Insertion of reactivity, leading to rising temperatures; **(2)** Due to relative changes in density with temperature, buoyancy effects act and the fuel rod is propelled upwards; **(3)** A subcriticality condition is reached, leading to falling temperatures; **(4)** Relative changes in density lead to loss of buoyancy and the fuel rod falls back down; **(5)** Fuel rod re-enters the core; **(6)** End of transient.

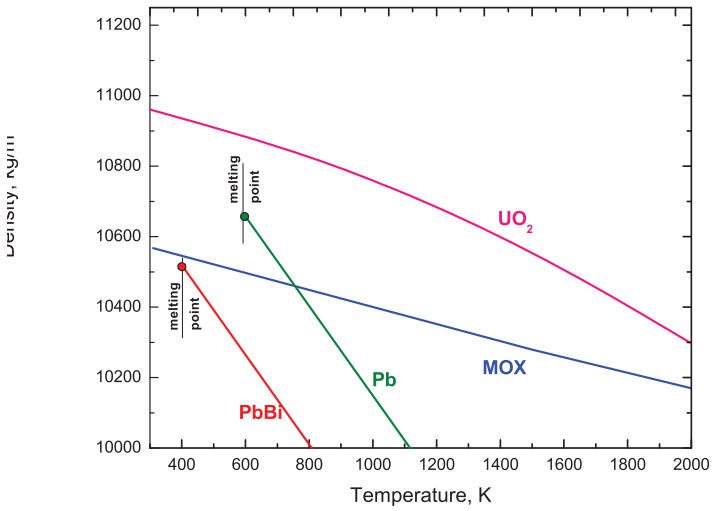

Fig. 2. Density variations of Pb-Bi eutectic and Pb coolants and MOX and UO_2 fuels as functions of temperature.

with temperature are not favorable. However, before deciding on the feasibility of the posited buoyancy mechanism, the fuel densities shown in Fig. 2 need to be corrected to account for the presence of stainless steel, mostly in the form of cladding. In this work, the profile temperature between fuel and coolant are the same as given in any available book on thermal analysis of nuclear reactors, and the fuel temperature is spatially averaged as indicated in the appendix.

To begin with, to take into account the effect of stainless steel on the total density of the fuel, a combined fuel-steel density may be defined as:

$$\bar{\rho}_f = F_f \rho_f + (1 - F_f)\rho_s \tag{1}$$

where F_f is the volume fraction of fuel and ρ_f and ρ_s are the densities of the fuel and stainless steel, respectively.

For practical purposes, the densities can be approximated as linear functions of temperature:

$$\rho_i = \rho_{i,0} - \alpha_i T_i \tag{2}$$

where the subscript i denotes the specific material, for example, $i = f$ for fuel, c for coolant, s for stainless steel, and $\rho_{i,0}$ is the density of material i at a temperature of 0 K, α_i is the rate of change of density of material i with temperature, and T_i is the temperature of material i in K. Then, the combined density given by Eq. (1) can be represented as a function of temperatures as:

$$\bar{\rho}_f = \bar{\rho}_{f,0} - \bar{\alpha}_f T_f \tag{3}$$

where

$$\bar{\rho}_{f,0} = [F_f \rho_{f,0} + (1 - F_f)\rho_{s,0}] \tag{4}$$

and

$$\bar{\alpha}_f = (1 - F_f)\frac{T_s}{T_f}\alpha_s \tag{5}$$

where the temperature T_s is the average temperature of cladding and can be calculated as $T_s = T_f - \Delta T$ being ΔT the temperature drop between fuel and cladding. This drop temperature is as above $\Delta T \approx 200$ K and for preliminary calculations has been used in this work.

From the available data in the literature, the linear relationships for fuels [17], coolants [16] and stainless steel [11] shown in Table 1 were formulated. All densities are given in kg m^{-3} for temperatures in K. The corresponding relationships are depicted in Fig. 3, where a volume fraction of stainless steel of 45.6% (from Table 2) was assumed.

Table 1. Assumed density variations with temperature.

Material type	**Material**	**Equation**
Coolant	Pb	$\rho_{\mathrm{Pb}} = 11478.69 - 1.32T_c$
Coolant	PbBi	$\rho_{\mathrm{PbBi}} = 11093.71 - 1.33T_c$
Fuel	UO_2	$\rho_{\mathrm{UO_2}} = 11122.84 - 0.36T_f$
Fuel	MOX	$\rho_{\mathrm{MOX}} = 10657.97 - 0.255T_f$
Cladding	Stainless steel SS-316	$\rho_s = 8077.729 - 0.42T_s$
Ballast	Tungsten	$\rho_w = 19300.0 - 0.22T_f$

Referring to Fig. 3, it can be seen the densities of the HLM coolants are consistently greater than those of the combined fuel-steel options. Thus, the desired buoyancy mechanism for self-ejection of a fuel rod will only be possible with the use of deadweight or ballast to increase the effective density of the fuel. The use of such ballast is discussed below.

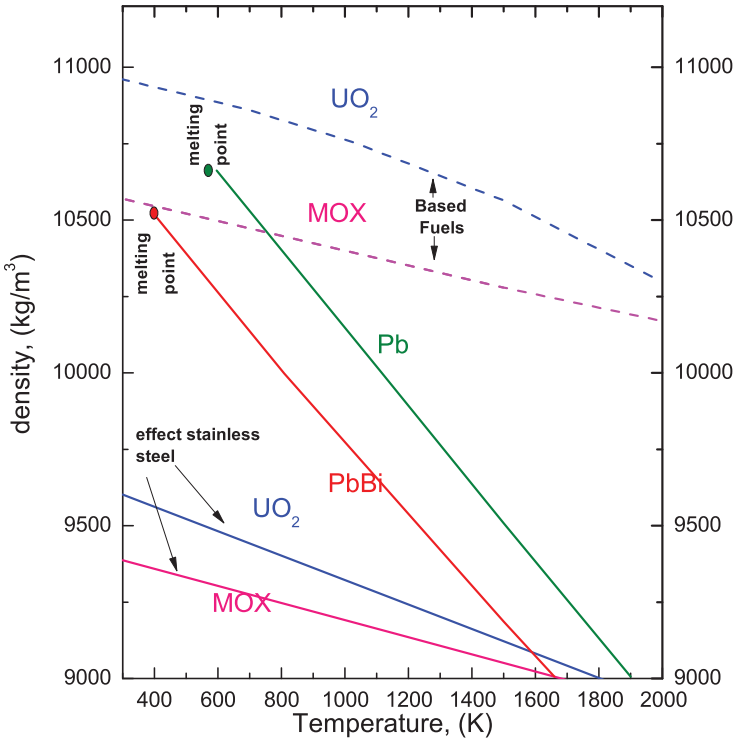

Fig. 3. Density variations as functions of temperature of Pb-Bi eutectic and Pb coolants and MOX- and UO_2-based fuels with a representative volume of stainless steel cladding.

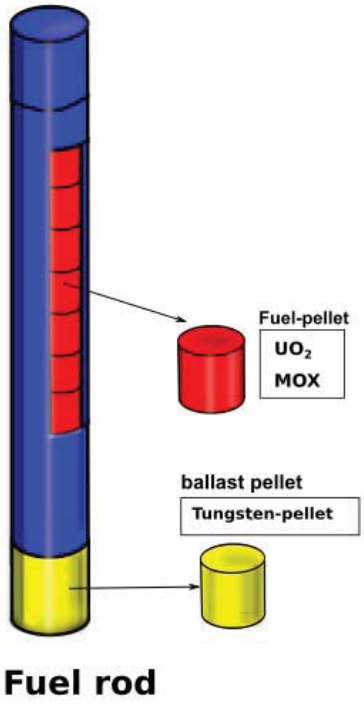

Fig. 4. The ballast pellet concept. In this concept buoyancy forces are harnessed to provide negative reactivity feedback by upward motion of the fuel element.

2.1. The tungsten ballast pellet

Although the use of tungsten as ballast in lead-cooled reactors has been proposed previously, its application was for a totally different purpose: tungsten ballast is located outside the core and used to keep the fuel assemblies in their designated positions by providing a downward force exceeding the force due to buoyancy under refueling conditions [1]. In other words, buoyancy forces are not contemplated as the basis of a feedback mechanism but, rather, they are neutralized over all temperatures by the use of an excess of ballast.

The proposed use of tungsten ballast here is with a totally different purpose in mind. We want to neutralize buoyancy, but only in the nominal range of working temperatures of the reactor, and we want buoyancy forces to appear if the nominal operating temperature range is exceeded, for example during a temperature or power transient. So, by introducing a tungsten ballast pellet occupying just the right volume within the fuel rod (as depicted in Fig. 4) we will be able to endow the fuel rod with a reliable mechanism for self-ejection or self-disassembly, as depicted in Fig. 1.

Our first step, therefore, is to derive an expression that allows us to determine what tungsten ballast pellet fraction will be needed, and our second step is to establish an initial estimate of the negative reactivity insertion arising from the consequent fuel rod self-ejection.

First, we need to define an "effective density" taking into account the volume fraction occupied by tungsten ballast pellets. Proceeding as in our previous analysis, the effective fuel-steel-tungsten density is:

$$\rho_{f,\text{eff}} = (1 - F_b)\bar{\rho}_f + F_b\rho_w \tag{6}$$

where F_b is the volume fraction of tungsten ballast used and ρ_w its density. From our foregoing discussion, Eq. (6) yields the following relationship:

$$\rho_{\text{eff}} = \rho_{\text{eff},0} - \alpha_{\text{eff}}T_f \tag{7}$$

where

$$\rho_{\text{eff},0} = (1 - F_b)\bar{\rho}_{f,0} + F_b\rho_{w,0} \tag{8}$$

For design considerations, it is desired a ballast pellet at the top or bottom of the fuel element avoiding thermal stresses between fuel pellets, also, it this way the ballast pellet can be used as reflector (due to high density of tungsten) and/or as a bottom-cap or top-cap as schematically sketched in Fig. 4. However, the location of this cap-ballast will be determined by the location of the gas plenum. If the gas plenum is in the same side than the ballast, then the ballast pellet should be endowed with holes allowing the free flow of fission gas toward the plenum.

In addition, as firs estimate of the the rate of negative reactivity insertion due to fuel ejection by buoyancy force in this preliminary work it will be evaluated using a uniform reactivity worth per displacement in the next sections. However, it is known that the axial distribution of fuel reactivity worth is approximately proportional to the axial power distribution, which is generally symmetric about the core mid-plane. Therefore, when a fuel pin is displaced upward by buoyancy force, the part of fuel displaced into higher power region introduces a positive reactivity while the part moved into a lower power region introduces a negative reactivity. As a result, an axial displacement of a fuel pin by buoyancy force may not introduce a large negative reactivity. Depending on the axial power shape, the net reactivity could be close to zero or even slightly positive. Nonetheless, the negative reactivity insertion due to fuel ejection by buoyancy force can be boosted by using a proper neutron-poison pellet as schematically depicted in Fig. 5.

Let us consider Fig. 4, as the most general case for application of the ballast pellet, this design -although rather simple, will allow us to get first

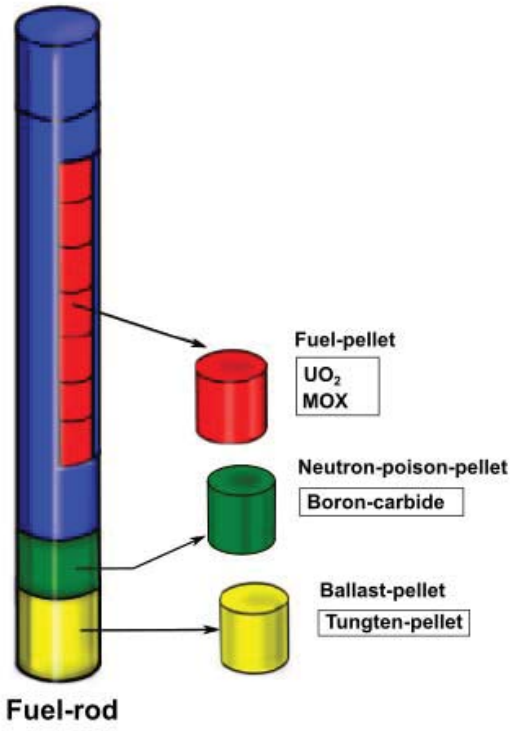

Fig. 5. The ballast pellet concept as depicted in Fig. 4 but with negative reactivity feedback effect boosted by the use of a neutron-poison pellet. When the fuel pin is displaced upward by buoyancy force also a neutronic poison is introduced in the core.

estimates on the feasibility of the concept and then to evaluate if it is worthy to pursue additional research/designs as depicted in Fig. 5.

Thus, taking the contribution of expansion of the ballast, the effective rate of change of density yields

$$\alpha_{\text{eff}} = (1 - F_b)\bar{\alpha}_f + F_b \frac{T_w}{T_f}\alpha_w \tag{9}$$

Where the temperature of the ballast T_w must be evaluated at this location. However, because the high thermal conductivity of tungsten ($\kappa_w \simeq 173\text{WK}^{-1}m^{-1}$) it could be assumed as the temperature of the fuel in the same region. The fuel temperature drops around a half between its maximum axial value (close to the center of the fuel element) and the outermost axial levels where the ballast should be placed. Thus, to be in the safe side, a conservative preliminary value for the effective ballast temperature is taken as $T_w \approx \frac{T_f}{2}$. Finally, a linear density-temperature relationship, as given by Eq. (2), was adopted for tungsten.

The latter assumption seems reasonable and appropriate given tungsten's high thermal conductivity, and also represents a conservative assumption, because, in overestimating the temperature of tungsten, we are underestimating

its density and thus overestimating the volume fraction needed. From the available literature [11], the density of tungsten fits the relationship given in Table 1.

Fuel rod ejection driven by buoyancy will only occur when the effective density of the fuel becomes lower than that of the surrounding coolant, or:

$$\rho_c > \rho_{\text{eff}} \tag{10}$$

To progress our analysis, we need an expression connecting the temperature of the fuel with the temperature of the coolant at the same instant in time. It should be noted, however, that even if the condition given by Eq. (10) is satisfied, this does not guarantee the feasibility of the proposed buoyancy mechanism: we must, additionally, be sure that this condition is accomplished at a power below the critical power that can jeopardize the structural integrity of the cladding. Thus, it is important to relate the fuel and coolant temperatures to the power being generated in the fuel. For transients in which reactivity ϱ is much lower than the delayed neutron fraction $\varrho \ll \beta$, the resulting reactor period would be considerably longer than the fuel thermal time constant τ given by [13]:

$$\tau \approx R_f M_f c_f \tag{11}$$

where M_f and c_f are the mass and specific heat capacity of the fuel, respectively, and R_f is the fuel thermal resistance given by:

$$R_f = \frac{1}{4\pi L \kappa_f} + \frac{1}{2\pi r_g L h_g} + \frac{1}{2\pi \kappa_s L} \ln\left(\frac{r_{s2}}{r_{s1}}\right) + \frac{1}{2\pi r_{s2} L h_c} \tag{12}$$

where κ_f is the thermal conductivity of the fuel, L the fuel rod length, r_g and h_g are the effective gap radius and heat transfer coefficient, respectively, r_{s2} and r_{s1} the outer and inner cladding radius, respectively, κ_s the thermal conductivity of the cladding, and h_c the coolant heat transfer coefficient. However, for oxide and mixed oxide fuel, the low thermal conductivity of the fuel is the limiting factor in the thermal resistance of the fuel, [14], and then, the fuel thermal time constant τ is simplified as $\tau \approx \frac{\rho_f c_f r_{s2}^2}{\kappa_f}$. Therefore, typical parameters for a UO_2 fuel element in a pin characteristic of a fast reactor with $r_{s2} = 0.25$ cm, the UO_2 fuel time constant would be about 6s. With a metal fuel instead of UO_2, where the heat conductivity of fuel is much larger, and the heat removal time are on the order of 0.1 to 1.0 s. [14]. In the

present work, for the thermal treatment we assume a mild transient, where mild transient is referred to a transient in which the reactor period is much larger than the thermal time constant.

It should be mentioned that Eq. (12) refers to the peak fuel temperature (centerline or hollow), not to the average fuel temperature. The latter is the temperature upon which density depends. A correction could be introduced by multiplying the first term in the right-hand side of Eq. (12) by $\frac{1}{2}$ [20]. However, the use of a peak fuel temperature, on one hand, results in an overestimation of the ballast pellet volume, but, on the other hand, in an underestimation of the power at which the buoyancy becomes effective. These effects will be somewhat compensatory, and, in view of the uncertainties in this preliminary assessment, let us use the peak fuel temperature in our calculations.

For the case where the reactor period is much longer than τ, the fuel and coolant temperatures can be expressed as functions of the power P as [13]:

$$T_f = \left[R_f + \frac{1}{2\dot{m}_c c_c} \right] P + T_i \tag{13}$$

and

$$T_c = \frac{1}{2\dot{m}_c c_c} P + T_i \tag{14}$$

where $\dot{m}_c$ and c_c are the coolant mass flow rate and heat capacity, respectively, and T_i the coolant inlet temperature.

Thus, using the equations above, we find that the point at which the condition given by Eq. (10) is met occurs at a power given by:

$$P^* = \frac{\rho_{c,0} - \rho_{\text{eff},0} - T_i \left(\alpha_c - \alpha_{\text{eff}} \right)}{\frac{\alpha_c - \alpha_{\text{eff}}}{2\dot{m}_c c_c} - \alpha_{\text{eff}} R_f} \tag{15}$$

To better understand the implications of these results, we assume some typical values for the relevant parameters. For the calculation of the thermal resistance, we take: $\kappa_f = 2$ $\text{Wm}^{-1}\text{K}^{-1}$, $\kappa_s = 15$ $\text{Wm}^{-1}\text{K}^{-1}$; from [15], $h_g = 5678.26$ $\text{Wm}^{-2}\text{K}^{-1}$, $h_c = 34069.58$ $\text{Wm}^{-2}\text{K}^{-1}$; and, from Table 2, $r_{s2} = 4.55$ mm, $r_{s1} = 3.4$ mm, with a core length of $L = 100$ cm. These result in a fuel thermal resistance of $R_f \approx 4.39 \times 10^{-2}$ KW^{-1}. For the coolant, we take $c_c = 160$ $\text{JK}^{-1}\text{kg}^{-1}$. The maximum coolant velocity allowed for lead-based coolants is on 2 $\text{m}\,\text{s}^{-1}$ because of issues of erosion [23].Then, for the channel dimensions given in Table 2, the coolant mass flow rate is $\dot{m}_c = 2$ $\text{kg}\,\text{s}^{-1}$.

Table 2. Design parameters of the HLMFR core concept considered, from [21].

Parameter	**Value**
Power	600 MW_e
Pellet outer radius	3.3 mm
Cladding inner radius	3.4 mm
Cladding outer radius	4.55 mm
Pitch-to-diameter ratio	1.5
Length of upper plenum	100 cm
Length of lower plenum	10 cm
Active pin length	100 cm
Pin-fuel volume fraction	54.4%
Pin-steel volume fraction	45.6%
Average linear pin power	11.5 kWm^{-1}

For the average nominal linear pin power, we take a value of 115 $W\,cm^{-1}$ as in table II. Taking an inlet temperature of $T_i = 750$ K, corresponding with a nominal linear pin power of 100 $W\,cm^{-1}$, then results in fuel and coolant temperatures that vary as functions of linear pin power as shown in Fig. 6.

Fig. 7 shows how the densities of Pb-Bi eutectic and Pb coolants will vary as functions of linear pin power according to these equations along with the variation of the effective density of MOX (Fig. 7) fuels. In these figures, the choice of the fraction of tungsten ballast pellets used was more or less arbitrary, with the only purpose being to obtain an estimate of the amount of ballast needed to stop the transient safely, i.e. to ensure that fuel rod ejection occurs at a linear power significantly smaller than a certain design constraint. For example, the current lead-bismuth cooled oxide-fuel reactor MYRRHA works with a nominal linear power of 370 $W\,cm^{-1}$, [7], and for other oxide fueled reactors a linear power up to 472 $W\,cm^{-1}$ limit is suggested [8]. However, as will be apparent to the reader, the nuclear designer has a certain freedom to choose over the maximum power at which the fuel rod is ejected. If the fraction of ballast is reduced from the values used in Fig. 7, ejection will start at a lower linear power, but the system will also become more sensitive to small changes of temperature.

Next, we need to obtain a first estimate of the amount of negative reactivity insertion caused by the buoyancy-driven ejection of the fuel rod when the Eq. (10) condition is met. This will be our objective in the next section.

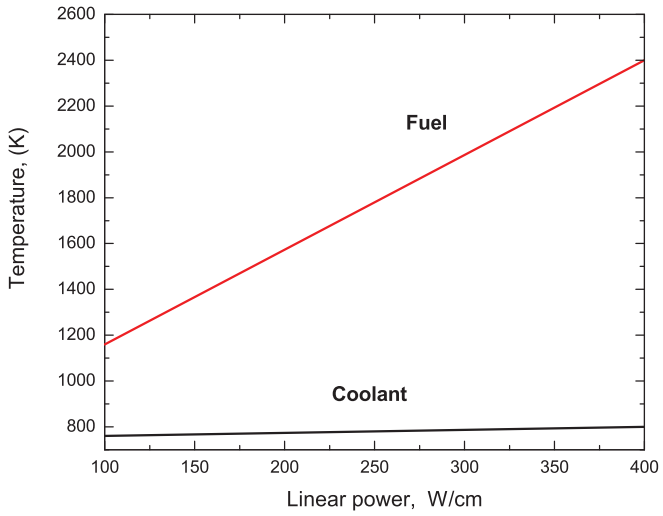

Fig. 6. Fuel and coolant temperatures as functions of linear pin power.

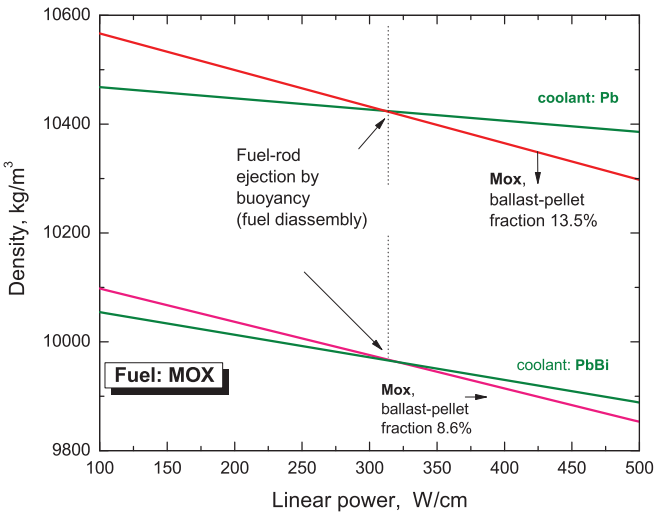

Fig. 7. Densities of coolants and MOX fuel as functions of linear pin power.

2.2. The negative reactivity insertion

At the moment fuel rod ejection starts the maximum reactivity is given by

$$\varrho_0 = \gamma_c \Delta T \tag{16}$$

where γ_c is the (positive) coolant temperature coefficient of reactivity and

$$\Delta T = T_c - T_c(0) \tag{17}$$

is the increase in coolant temperature from the initial value $T_c(0)$ to the temperature T_c when ejection occurs, i.e. at power $P = P^*$.

The negative reactivity insertion due to the sudden upward motion of the fuel rod over a small time-step Δt is:

$$\Delta\varrho = -\left|\frac{\partial\varrho}{\partial z}\right|\left|\frac{\partial z}{\partial t}\right|\Delta t = -\left|\frac{\partial\varrho}{\partial z}\right| V_t \Delta t \tag{18}$$

where V_t is approximately the terminal velocity of the cylindrical fuel rod, given by [12]:

$$V_t = \sqrt{\frac{2gL}{C_d}} B \tag{19}$$

where g is the acceleration due to gravity, L is the fuel rod length, C_d is the drag coefficient, and B is a buoyancy-driving parameter defined as:

$$B = \sqrt{\frac{\rho_c - \rho_{\text{eff}}}{\rho_c}} \tag{20}$$

Using the representative values specified in the previous section, the relationship between B and linear pin power for lead coolant and UO_2 fuel is as shown in Fig. 8.

Now, in sufficiently slow transients, as soon as the condition given by Eq. (10) is satisfied, there will be a small prompt jump in power, but then the system will come to equilibrium as the rise in fuel and coolant temperatures and the increase in B compensate for ϱ_0, sending $\varrho(t) \to 0$. Because we are interested in knowing the separated effect of buoyancy in the negative feedback and then be able to evaluate if it is worthy the mechanism, let us omit the Doppler effect, and in this way evaluating the separated effect of the buoyancy and simultaneously performing a very conservative estimation which in view of several uncertainties in the calculations seems preferable.

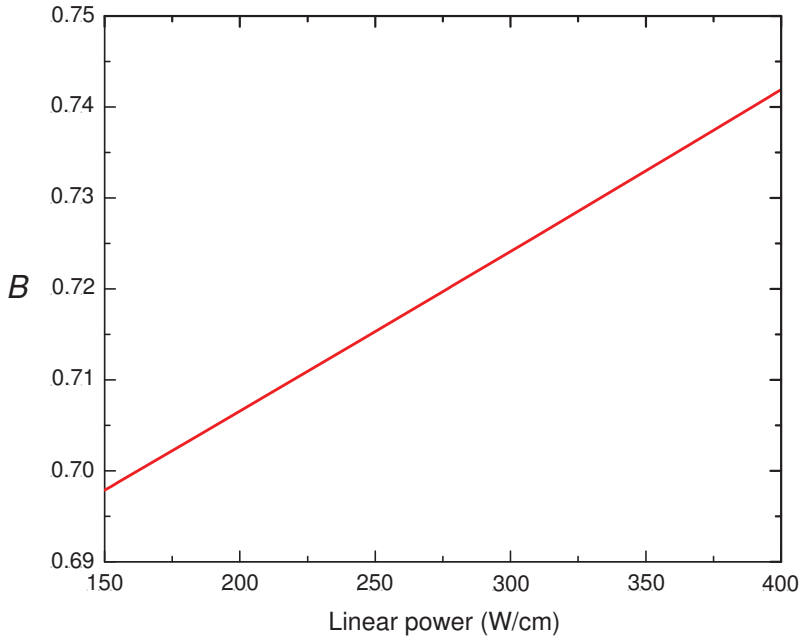

Fig. 8. The buoyancy-driving parameter B with lead coolant and UO_2 fuel as a function of linear pin power.

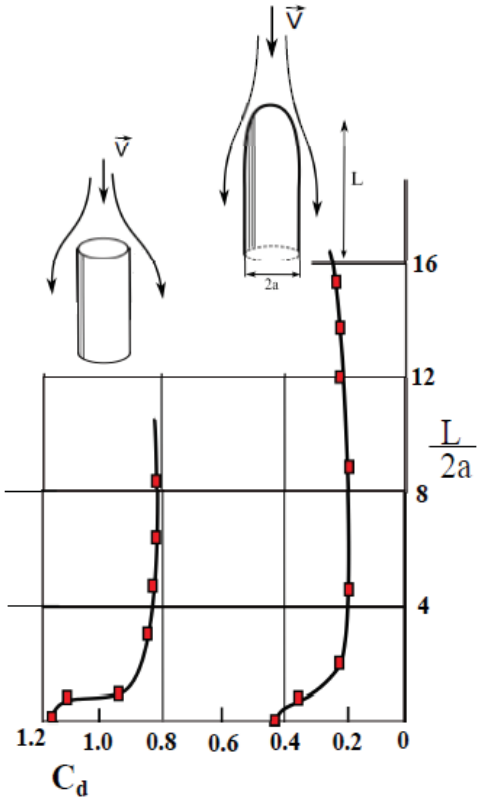

Fig. 9. Drag coefficients of blunt-nosed and rounded-nosed cylinders versus fineness ratio $L/2a$ [9].

Thus, the new equilibrium power will be given by [13]:

$$P(\infty) = P^* + 2\dot{m}_c c_c \left[\frac{\varrho_o}{\gamma_c}\right] \tag{21}$$

Using the power $P(\infty)$ we can calculate the coolant and fuel temperatures from Eqs. (13) and (14) and then their respective densities. This then allows us to find the value of the buoyancy parameter B given by Eq. (20). For example, taking $\Delta T = \varrho_o/\gamma_c \approx 5$ K, we obtain an approximate value for $B \approx 0.1$. The drag coefficient C_d will be between 1.2 for a blunt-nosed cylinder or 0.2 for a rounded nose, as shown in Fig. 9 [9]. Thus, for an optimized fuel rod with a rounded end-cap, as depicted in Fig. 10, we can assume $C_d = 0.2$, and with a total fuel rod length (including plenums) of 210 cm (see Table 2), we obtain a terminal velocity of $V_t \approx 1.44\ \mathrm{m\,s^{-1}}$.

Finally, we need an estimate of the variation of reactivity with the displacement of the ejected fuel rod, i.e. $\partial\varrho/\partial z$. Unfortunately, this is a highly uncertain parameter; its accurate computation requires knowledge of the specific location at which the fuel rod ejection occurs, as well as the specific design of the rod. A calculation performed using the SCALE 6 software [4] for a typical fuel rod channel, using lead as the coolant and reflective

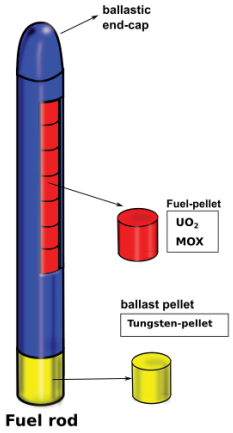

Fig. 10. A possible optimized fuel rod design for a lead or lead-bismuth cooled reactor. The end-cap is rounded to enhance the ejection velocity.

boundary conditions surrounding the channel, provides us with a conservative value of $\partial\varrho/\partial z \approx -50$ pcm cm^{-1}. Then using our previously calculated estimate of the fuel rod terminal velocity, we have a rate of negative insertion on -7200 pcm s^{-1}. Taking a typical positive coolant temperature coefficient of reactivity to be 0.36 pcm K^{-1} [21] and $\Delta T = 5$ K, the time needed for the buoyancy-driven mechanism to control this transient will be a tiny fraction of a second once the Eq.(10) is met.

Thus, the foregoing calculations indicate that by using a modest fraction ($\sim$15%) of tungsten ballast pellets the fuel rod will be endowed with a reliable self-ejection mechanism during temperature transients. It should be noted that, in these preliminary calculations, other components of the fuel rod which can reduce its effective density even more were neglected, the most important being the gas plenum chambers (if fission gases are not vented directly into the coolant). However, the potential reduction in the effective fuel rod density due to the gas plenums can be compensated by using tungsten rather than stainless steel for the lower and upper plenums in the fuel rod.

3. Conclusions

In this paper we explored the possibility of taking advantage of buoyancy forces in heavy liquid metal cooled fast reactors to endow the fuel rod with a reliable and passive negative feedback mechanism through fuel rod

ejection (a fuel self-disassembly mechanism) during a temperature transient, compensating the positive coolant temperature coefficient of reactivity that many fast reactors feature. It was deduced that, through the use of tungsten ballast pellets introduced into the fuel rod, such a mechanism is feasible, with the volume occupied by the ballast pellets being less than 15%.

This preliminary assessment was based on unavoidable idealizations, some conservative and others non-conservative. It should not be misconstrued as a definitive, detailed analysis. Additional R&D is required to further explore the possibilities of this concept, to seek optimal values for the design variables, and to determine real practical applicability as details are refined. Only then will the feasibility of the proposed concept be fully established.

4. Appendix

4.1. The fuel element motion

As mentioned in preceding sections, the proposed mechanism implies that fuel rods must be capable of moving by buoyancy force, which means that the fuel rods are not fixed and will need some sort of spring system to keep the position, and can move more easily by the change of coolant velocity, and as a result the vertical positions of fuel rods could change with the change of the coolant velocity in the reactor core. a situation which cannot be desired by the nuclear engineer.

Fortunately, in order to do so, the dynamic pressure exerted by the coolant motion to the fuel element should be in the same order than the weight of the fuel element itself. The above condition implies the following mathematical condition

$$\frac{\rho_c C_d V^2 A_f}{\rho_f V_f g} \geq 1 \tag{22}$$

where the term in the numerator is the coolant dynamic pressure exerted by the coolant with a density ρ_c drag coefficient C_D, velocity V and a projected area of the fuel element A_F. The denominator is the weight of the fuel element where ρ_f is the density of the fuel, V_f the volume of the fuel element and g is gravity. if we are considering a cylindrical fuel element with $A_f = \pi R_f^2$ and $V_f = A_f l_f$ where R_F is the radius of the fuel element and l_f its length, and also considering that for a HLMFR $\rho_c \approx \rho_f$, then Eq.(22) is

simplified as

$$\frac{C_d V^2}{l_f g} \geq 1 \tag{23}$$

with $C_D = 0.5$; with a maximum coolant velocity $V < 1\text{m/s}$; $l_f \simeq 2\text{m}$ and with $g = 9.8\ \text{m/s}^2$, we have

$$\frac{C_d V^2}{l_f g} \approx 2.5 \times 10^{-2} \tag{24}$$

Therefore, in order to accomplish the condition given by Eq.(23) and then the motion of the coolant translate in motion of the fuel, the nominal velocity should be increased a factor 10. However, the pumping power is scaled with the velocity as $\propto V^3$, [22] i.e., that the pumping power should be increased a factor 1000 in order to increase the velocity of the coolant a factor 10. In view of the above estimation the problem of the motion of the fuel by the motion of the coolant can be justifiable neglected.

4.2. The average fuel temperature

In previous sections it was used a fuel temperature which is the average fuel temperature which results in the average density of the fuel which is the parameter of importance for calculation of the onset of buoyancy. The average density of the fuel is calculated as

$$\rho_f \approx \frac{1}{R_f^2} \int_0^{R_f} 2\rho_f(R) R dR \tag{25}$$

Once the average density is calculated the corresponding fuel temperature is also obtained

Nomenclature

B = buoyancy parameter defined by Eq. (20)
C_d = drag coefficient
c_i = heat capacity of material i
F_f = volume fraction of fuel
g = acceleration due to gravity
h = heat transfer coefficient
L = length (of fuel pin or fuel rod)

$\dot{m}_c$ = coolant mass flow
M_f = mass of fuel
P = pin power
P^* = pin power at onset of rod ejection
r = radius
R_f = thermal resistance of fuel pin
t = time
T = temperature
T_i = inlet temperature of coolant
V_t = terminal velocity
z = vertical coordinate

Greek symbols

α_i = rate of change of density of material i with temperature
β = fraction of delayed neutrons
γ_c = coolant temperature coefficient of reactivity
κ_i = thermal conductivity of material i
ρ_i = density of material i
τ = the fuel thermal time constant
ϱ = reactivity

Subscripts

c = coolant
f = fuel
g = gap
s = stainless steel
w = tungsten

ACKNOWLEDGEMENTS

This research was supported by the Spanish Ministry of Economy and Competitiveness under fellowship grant Ramon y Cajal: RYC-2013-13459.

References

[1] Alemberti, A., 2012. The European lead fast reactor: design, safety approach and safety characteristics. In: IAEA Technical Meeting on Impact of Fukushima Event on Current and Future FR Designs, Dresden,

Germany. http://www.iaea.org/NuclearPower/Meetings/2012/2012-03-19-03-23-TM-NPTD.html

[2] Alessandro, A., 2014. Final Report Summary - LEADER (Lead-cooled European Advanced Demonstration Reactor). European Commission Community Research and Development Information Service. http://cordis.europa.eu/result/rcn/147643_en.html

[3] Arias, F.J., 2014. The phenomenology of packed beds in heavy liquid metal fast reactors during postaccident heat removal: The self-removal feedback mechanism. Nucl. Sci. Eng. 178(2), 240–249.

[4] Bowman, S.M., 2011. SCALE 6: Comprehensive nuclear safety analysis code system. Nucl. Technol. 174(2), 126–148.

[5] Cacuci, D.G., 2010. Handbook of Nuclear Engineering: Volume 1: Nuclear Engineering Fundamentals. Springer, New York, NY.

[6] Di Maio, D.V., Cretara, L., Giannetti, F., Peluso, V., Gandini, A., Manni, F., Caruso, G., 2014. An alternative solution for heavy liquid metal cooled reactors fuel assemblies. Nucl. Eng. Des. 278, 503–514.

[7] Jaluvka D., 2015. Development of a Core Management Tool for the MYRRHA Irradiation Research Facility. Doctoral Dissertation.

[8] Ganda, F., Arias, F.J., Vujic, J., Greenspan, E., 2012. Self-sustaining thorium boiling water reactors. Sustainability 4, 2472–2497.

[9] Hart, R.G., 1955. Flight investigation at Mach numbers from 0.8 to 1.5 to determine the effects of nose bluntness on the total drag of two fin-stabilized bodies of revolution. Technical note 3549. National Advisory Committee for Aeronautics NACA.

[10] Hejzlar, P., Driscoll, M.J. Kazimi, M.S., 2002. Conceptual Reactor Physics Design of a Lead-Bismuth-Cooled Critical Actinide Burner. Technical report MIT-ANP;TR-069. Massachusetts Institute of Technology Advanced Nuclear Power Technology Program, Cambridge, MA.

[11] Inco Databooks, 1968. Austenitic Chromium-Nickel Stainless Steels at Elevated Temperatures – Mechanical and Physical Properties (2980). Available from http://www.nickelinstitute.org/.

[12] Janna, W.S., 2010. Introduction to Fluid Mechanics. Fourth Edition. CRC Press, Boca Raton, FL.

[13] Lewis, E.E., 1977. Nuclear Power Reactor Safety. John Wiley and Sons, New York, NY.

[14] Weston M. Stacey. 2007. Nuclear Reactor Physics. 2nd Edition. Wiley-VCH Verlach GmbH & Co. KGaA.

[15] Massoud, M., 2005. Engineering Thermofluids: Thermodynamics, Fluid Mechanics, and Heat Transfer. Springer-Verlag, Berlin, Heidelberg, Germany.

[16] Nuclear Energy Agency, 2007. Handbook on Lead-bismuth Eutectic Alloy and Lead Properties, Materials Compatibility, Thermal-hydraulics and Technologies. https://www.oecd-nea.org/science/reports/2007/nea6195-handbook.html

[17] Popov, S.G., Carbajo, J.J., Ivanov, V.K., Yoder, G.L., 2000. Thermophysical Properties of MOX and UO_2 Fuels Including the Effects of irradiation. Technical report ORNL/TM-2000/351. Oak Ridge National Laboratory, Oak Ridge, TN.

[18] Qvist, S., Greenspan, E., 2014. An autonomous reactivity control system for improved fast reactor safety. Prog. Nucl. Energy. 77, 32–47.

[19] Ronchi, C., Sheindlin, M., Staicu, D., Kinoshita, M., 2004. Effect of burn-up on the thermal conductivity of uranium dioxide up to 100.000 MWdt-1. J. Nucl. Mater. 327 (1), 58-76.

[20] Todreas, N.E., Kazimi, M.S., 2011. Nuclear Systems Volume I: Thermal Hydraulic Fundamentals. Second edition. CRC Press, Boca Raton, FL.

[21] Tuček, K., Carlsson, J., Wider, H., 2006. Comparison of sodium and lead-cooled fast reactors regarding reactor physics aspects, severe safety and economical issues. Nucl. Eng. Des. 236, 1589–1598.

[22] Waltar, A.E., Reynolds, A.B., 1981. Fast Breeder Reactors. Pergamon Press, Elmsford, NY.

[23] Zhang, J., Li, N., 2008. Review of the studies on fundamental issues in LBE corrosion. J. Nucl. Mater. 373 (1–3), 351–377.